1 OF 1
ADA048 411

END
DATE
FILMED
2 -78
DDC

NPS-67Nt77092

NAVAL POSTGRADUATE SCHOOL
Monterey, California

DDC
RECEIVED
JAN 17 1978
B

AN INVESTIGATION OF THE COMBUSTION BEHAVIOR

OF

SOLID FUEL RAMJETS

C. J. Mady, P. J. Hickey, D. W. Netzer

September 1977

NAVAL POSTGRADUATE SCHOOL

Monterey, California

Rear Admiral I. W. Linder   Jack R. Borsting
Superintendent   Provost
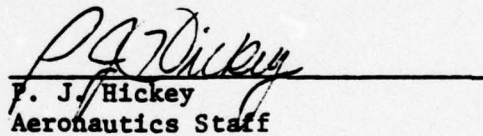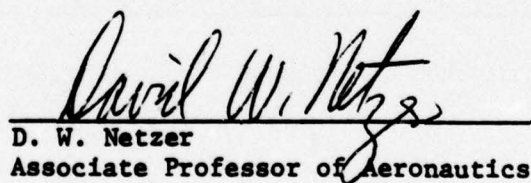
Reproduction of all or part of this report is authorized.

This report was prepared by:

C. J. Mady, Jr

C. J. Mady
LT, USN

P. J. Hickey

P. J. Hickey
Aeronautics Staff

D. W. Netzer

D. W. Netzer
Associate Professor of Aeronautics

Reviewed by: Released by:

R. W. Bell   _R. R. Fossum_

R. W. BELL, Chairman   R. R. FOSSUM
Department of Aeronautics   Dean of Research

i

SECURITY CLASSIFICATION OF THIS PAGE (When Data Entered)

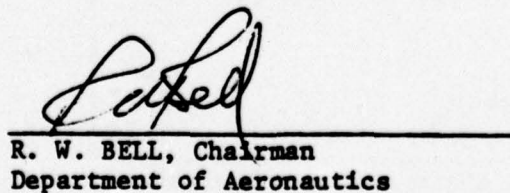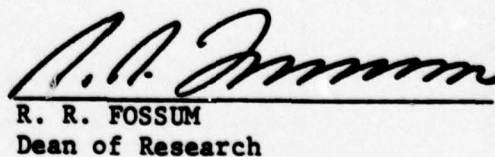| REPORT DOCUMENTATION PAGE		READ INSTRUCTIONS BEFORE COMPLETING FORM
1. REPORT NUMBER NPS-67Nt77092	2. GOVT ACCESSION NO.	3. RECIPIENT'S CATALOG NUMBER
4. TITLE (and Subtitle) AN INVESTIGATION OF THE COMBUSTION Behavior OF SOLID FUEL RAMJETS.		5. TYPE OF REPORT & PERIOD COVERED Interim rept. '78
		6. PERFORMING ORG. REPORT NUMBER
7. AUTHOR(s) Clemens J. Mady, Jr., P. J. Hickey David W. Netzer		8. CONTRACT OR GRANT NUMBER(s)
9. PERFORMING ORGANIZATION NAME AND ADDRESS Naval Postgraduate School Monterey, CA 93940		10. PROGRAM ELEMENT, PROJECT, TASK AREA & WORK UNIT NUMBERS 62331N; F31300 N60530 - 77WR30051
11. CONTROLLING OFFICE NAME AND ADDRESS Naval Weapons Center China Lake, CA		12. REPORT DATE Sep 77
		13. NUMBER OF PAGES 48 p.
14. MONITORING AGENCY NAME & ADDRESS(if different from Controlling Office)		15. SECURITY CLASS. (of this report) UNCLASSIFIED
		15a. DECLASSIFICATION/DOWNGRADING SCHEDULE

16. DISTRIBUTION STATEMENT (of this Report)

Approved for public release; distribution unlimited

17. DISTRIBUTION STATEMENT (of the abstract entered in Block 20, if different from Report)

18. SUPPLEMENTARY NOTES

19. KEY WORDS (Continue on reverse side if necessary and identify by block number)

Ramjets
Solid Fuel
Combustion
Model

20. ABSTRACT (Continue on reverse side if necessary and identify by block number)

An experimental and analytical investigation was conducted of the combustion behavior in solid fuel ramjets. The effects of configuration variables on combustion performance were experimentally determined. Air ducting methods were found to affect combustion efficiency through fuel port flow rates, bypass dump momentum and geometry and bypass ratio. Bypass configurations with plexiglas fuel altered the heat transfer mechanisms within the port and decreased combustion efficiency. The analytical model was found to be in qualitative agreement

DD FORM 1473 EDITION OF 1 NOV 65 IS OBSOLETE
1 JAN 73
(Page 1)   S/N 0102-014-6601 |

UNCLASSIFIED
SECURITY CLASSIFICATION OF THIS PAGE (When Data Entered)

with experimental data. Finite rate kinetics and radiative transfer to the fuel surface will be required in the model to obtain more quantitative accuracy.

DD Form 1473 (BACK)
1 Jan 73
S/N 0102-014-6601

111

UNCLASSIFIED
SECURITY CLASSIFICATION OF THIS PAGE(When Data Entered)

TABLE OF CONTENTS

1

LIST OF TABLES

LIST OF FIGURES

3

I. NOMENCLATURE

A_i = Cross-sectional area of inlet to fuel grain

A_p = Cross-sectional area of fuel grain

B = Mass transfer parameter, $(h_p - h_o)/h_o - h_T)$

C_1, C_2 = Coefficients in $k-\epsilon$ turbulence model

C_p = Specific heat at constant pressure

C_{fo} = Friction coefficient without mass addition

D_p = Inside diameter of fuel grain

G = Generation term in equations for k and ϵ ,

$$\mu_{eff} \left\{ 2\left[\left(\frac{\partial v_z}{\partial z}\right)^2 + \left(\frac{\partial v_r}{\partial r}\right)^2 + \left(\frac{v_r}{r}\right)^2 \right] + \left(\frac{\partial v_z}{\partial r} + \frac{\partial v_r}{\partial z}\right)^2 \right\}$$

G_{air} = Mass flux of air based on bulk velocity

h = Enthalpy, $C_p (T - T^\circ) + m_{ox} H_o/i$

H_o = Effective heat of combustion, cal/gm of fuel

i = Stoichiometric ratio of oxygen mass to fuel mass

k = Turbulence kinetic energy

ℓ_p = "Length scale" of eddies at near wall grid point P

L_p = Length of fuel grain

m = Mass fraction

$\dot{m}''$ = Mass flux from fuel surface

$\bar{M}$ = Average molecular weight

p = Pressure

P_r = Molecular Prandtl number

r = Radial coordinate

$\dot{r}$ = Regression rate of fuel surface

R = Universal gas constant

R_e = Near wall grid Reynolds number, $\bar{\rho} \bar{v} y_p/\mu_o$

4

R_P = Internal radius of fuel port

R_t = Turbulent Reynolds number, $k_P^{1/2} y_P \rho/\mu_o$

S_ϕ = Source term in differential equation for generalized dependent variable ϕ

T = Temperature

V = Velocity

y_P = Distance from wall to near wall grid point P

y_P^+ = Non-dimensionalized distance from wall, $(\rho/\mu_o)(\tau_o/\rho)^{1/2} y_P$

z = Axial coordinate

γ = Slip function from Couette flow for boundary condition on k

ε = Rate of dissipation of turbulence energy

η = Combustion Efficiency based on total temperature rise across combustor

μ = Molecular viscosity

μ_{eff} = Turbulent viscosity

ρ = Density

σ_{eff} = Effective turbulent Prandtl or Schmidt number

τ = Shear stress

ϕ = Generalized dependent variable

ψ = Stream function

ω = Vorticity

Subscripts

fu = Fuel

h = Enthalpy

N_2 = Nitrogen

o,w = Wall

of = Refers to the "property" $m_{fu} - m_{ox}/i$

5

ox   = Oxygen

P   = Near wall grid point

r   = Radial component

T   = Reference condition deep within fuel grain

z   = Axial component

θ   = Tangential component

Superscripts

o   = Reference conditions

−   = Average value

II. INTRODUCTION

Several characteristics of the solid fuel ramjet indicate that it may be superior to other forms of propulsion for tactical weapons used at intermediate ranges and high speed. Having no moving parts, the solid fuel ramjet is simple and relatively inexpensive to fabricate. Weight of the system and its threat as a fire hazard are both decreased by use of the solid fuel.

To be used in a tactical situation, the solid fuel ramjet has to demonstrate combustion stability and efficiency over the expected operating envelope of altitudes and Mach numbers. It must also show performance comparable to that of liquid fuel ramjets and ducted rockets.

Combustion studies on the solid fuel ramjet have been underway at United Technologies-Chemical Systems Division since 1971. Initial work showed low temperature rise combustion efficiencies. The discovery of the rearward facing step at the combustor entrance as a flameholder was a significant gain in solid fuel ramjet technology. Overall performance, however, was reduced by the high stagnation pressure loss produced by the rearward facing step. Further work by United Technologies in the field of flame stabilization involved various inlet designs including aerogrids, distorted flows, noncircular inlets and vortex generators. This effort led to the development of inlets which minimized the required inlet step height and decreased the effects of inlet distortion.

Work was also underway at the Naval Postgraduate School on the internal ballistics of the solid fuel ramjet. Early work[1] showed that inlet turbulence and distortion may have a significant effect on flame stability.

The solid fuel ramjet, which uses air as the oxidizing agent, is similar to the hybrid rocket and has two distinct combustion zones within the fuel grain (Fig. 1). Behind the step is the recirculation zone where an intense

7

mixing of reactants and products takes place. The hot products ignite the reactant and combustion may in the limiting case approach that of a well-stirred reactor. This combustion region acts as the flame initiator for the combustion which takes place further down the fuel grain.

Downstream of the flow reattachment point a boundary layer develops. Here combustion is similar to that of the hybrid rocket. A diffusion flame exists in the developing turbulent boundary layer between the fuel rich zone near the wall and the oxygen rich central air core. Heat is transported by convection and radiation to the solid surface which causes decomposition of the fuel. Studies have shown that the rate of decomposition of the fuel is sensitive to the combustion pressure, the inlet air temperature and the mass flux of the air. Finite rate kinetics may be of importance for certain fuels and operating environments.

The combustion process in the solid fuel ramjet is thought to be mixing limited at combustion pressures greater than 10-15 psia for all-hydrocarbon fuels. However, this remains to be verified and other fuels have demon-strated behavior more characteristic of kinetically controlled combustion.

Unburned gaseous fuel escapes from under the flame at the aft end of the fuel grain and results in decreased combustion efficiency. This resulted in the use of a mixing chamber downstream of the fuel grain. Temperature rise efficiencies have been found to be a function of the rate of mixing between the fuel rich boundary layer and the cental air core. Too rapid mixing may quench the chemical reactions and further reduce combustion efficiency. Two somewhat distinct combustion zones also exist in the aft mixing section, the recirculation zone formed by the fuel grain or aft orifice and the central core zone.

8

The use of aft-end mixing devices to improve combustion efficiency is an area of recent interest in solid fuel ramjet technology. As another means of promoting mixing, the bypassing of a portion of the inlet air around the fuel grain and dumping it into the aft mixing chamber is being re-evaluated. A meteorlogical sounding rocket capable of an altitude of 200,000 feet was designed and built by Anderson, Greenwood and Company, Houston, Texas in 1961[2]. The MET JET employed a ramjet using a magnesium and magnesium-aluminum alloy epoxy-metal charge. Eighty-five percent of the inlet air was bypassed around the fuel grain to mix in an afterburner section with the fuel rich primary flow.

In the bypass systems the flow rates into the fuel grain inlet and aft mixing section are critical factors in determining combustion efficiency. Bypass air flow of too low a percentage of the total air mass flow or of too low momentum may have negligible effect on the combustion efficiency. Bypass air of too high a flow rate or momentum may have a negative effect on the combustion process. The bypass air is of appreciably lower temperature than the species which exit from the fuel grain, and air injected at too high a rate may cool the process sufficiently to affect the kinetics of the reaction. Furthermore, the combustion process in the aft mixing chamber may also be a function of the axial and radial positions and the angular orientations of the aft dumps.

This experimental investigation considered the effects of bypass configuration and operating conditions on the combustion behavior of a solid fuel ramjet which utilized polymethylmethacrylate as the fuel.

In order to guide development efforts and to provide needed input to systems analysis studies, combustion models are needed which can predict the fuel regression rate, flammability limits and combustion efficiency as a

9

function of hardware design and operating environment.

Modeling efforts for the combustion process in solid fuel ramjets have proceeded along two directions. Dunlap[3] has developed a semi-empirical regression rate model which is based upon reacting turbulent boundary layer theory and experimentally obtained wall heat transfer rates in non-reacting flows. Work at the Naval Postgraduate School[1,4] has been directed toward adaptation of the Spalding, et al model[5,6] for heat and mass transfer in recirculating flows to the SFRJ geometry.

Experimental data[3] have shown that the recirculation zone is fuel rich and that the primary combustion region (or flame zone) spreads out from along the shear layer between the recirculation zone and the inlet flow. The flame has been observed to be quite broad near the flow reattachment position and subsequently develops into a turbulent diffusion flame within the developing boundary layer downstream of reattachment.

The initial modeling work at the Naval Postgraduate School considered the effects of finite rate kinetics and combustor geometry on the flame pattern and internal flow field.

Several weaknesses were evident in the earlier work. Fuel regression rates were not calculated. Also, the flame pattern was not in agreement with experimental data, i.e., the recirculation region was predicted to be oxidizer rich and the flame within the boundary layer region spread too rapidly toward the centerline of the motor. In addition, the model had not been adequately checked for accuracy against experimental data for velocity, pressure and turbulence intensity.

The present investigation was conducted to improve the qualitative accuracy of the model, to incorporate prediction of the fuel regression rate, and to check the validity of the model against experimental data.

10

The majority of the analytical studies were conducted for polymethyl-methacrylate (PMM) fuel. PMM-air combustion produces minimal radiative heat transfer to the fuel grain for high mass flow rates through the port. The latter condition is characteristic of non-bypass systems. The model developed for this system did not include radiative heat transfer or finite rate kinetics.

The current investigation also considered the application of the model to the combustion behavior of all-hydrocarbon fuels which exhibit significant gas-phase radiation. In particular, model predictions were compared to the data obtained by Schadow[7].

III. EXPERIMENTAL INVESTIGATION

A. Equipment and Procedures

A schematic of the solid fuel ramjet is shown in Fig. 2. The apparatus employed a fuel port to dump inlet area ratio of 9.0 and a fuel port to nozzle throat area ratio of 4.0. The exit area of the grain (for most tests conducted) was held fixed at the initial port area by using a thin orifice plate. The aft mixing chamber had a length to diameter ratio (L/D) of 2.93. The aft mixing chamber consisted of three interchangeable sections such that the axial location of the bypass dump could be varied. One section contained four inlets for the bypass air. The inlet diameters were 2.70 cm with plugs available to reduce the diameters to 2.065, 1.908, 1.458, or 0.635 cm, or to seal the inlets off entirely. An additional section was fabricated which pro-vided bypass dumps oriented tangentially to the mixing chamber wall and perpendicular to its centerline. In most tests conducted the bypass dump was located in the forward position, within the recirculation zone of the aft mixing chamber.

11

All test firings were performed in the jet engine test cell at the Naval Postgraduate School. Data for calculating temperature rise efficiencies based on combustion pressure were obtained while varying primary and bypass air flow rates and bypass dump geometry. Nominal air flow rates were 0.1 and 0.2 lbm/sec for non-bypass runs and 0.2 lbm/sec for runs using bypass. A summary of the test conditions are presented in Table I.

Table I   Summary of Experimental Conditions

Air Inlet Temperature (°K): 292, 389

Bypass Dump Location: forward and aft of flow reattachment

Bypass (% Port/% Bypass): 100/0, 65/35, 50/50. 35/65

Momentum Ratio (Dump/Port)
  for 50/50 Bypass: 0.3, 0.5, 0.6, 1.0, 5.3

Dump Configuration: none, 2 at 180°, 2 at 90°, 4 at 90°, 2 at 180° with swirl

The majority of the test firings were made using a nominal inlet air temperature of 70°F. For those using the air heater (non-vitiated air), two to three hours were allowed for the temperature to stabilize at the ramjet inlet and in the bypass air line.

The weight, length and inside diameter of the fuel grains were measured prior to being mounted in the motor. The ignition sequence normally lasted for six seconds. An average of three seconds was required for the ignition flame to propagate from the head-end assembly into the fuel grain. After five seconds, the air was directed through the ramjet motor. Ignition was continued into the first second of the run to insure that combustion would be sustained. Total time of the ignition flame in contact with the fuel grain amounted to approximately three seconds. Two tests were made using only the ignition system in order to determine the rate of consumption of

12

the PMM grains during the oxygen-methane ignition. These data were used to correct the initial weight of the fuel used in the efficiency calculation.

Combustion normally lasted for forty-five seconds. The motor was extinguished at the end of each run by simultaneously venting the air to the atmosphere and actuating the nitrogen purge system. Low pressure air was then blown through the motor for cooling.

Thirty-three hot firing PMM tests were conducted. Combustion efficiencies were based on the total temperature rise from just upstream of the rearward facing step at the fuel port inlet to the nozzle inlet. Inlet total temperature was derived from the measured inlet static temperature. Actual combustion temperature was derived from the measured static pressure in the aft mixer.

Regression rate was calculated based on weight loss of the fuel. The inside diameter of the aft end of the fuel grain was also measured before and after each firing. However, as observed by Boaz and Netzer[8], it was found that weight loss gave a more consistent value of regression rate than the method based on aft end diameter change, due to the non-uniform regression along the length of the grain.

The calculated temperature rise efficiencies based on pressure are prone to error, since uncertainty in efficiency varies as the square of the uncertainty in the pressure measurement. Errors as large as 7% were possible. However, the uncertainty in percent theoretical C* was approximately 2% and the temperature rise efficiencies followed the C* efficiencies within 1.5%.

B. Results and Discussion

(a) Regression Rate

Several runs were made without using bypass air. These showed the dependence of the regression rate, $\dot{r}$ (in/sec) on combustion pressure, P (psia)

13

and average mass flux of air, G_{air} (lbm/in^2-sec) to be:

$$\dot{r} = 0.0043 P^{.29} G_{air}^{.38} \tag{1}$$

A plot of the regression rate versus this empirical regression rate equation
for the 0.2 and 0.1 lbm/sec non-bypass runs made with cold inlet air is
shown in Fig. 3.

In their work with PMM, Boaz and Netzer[8] had shown a regression rate
dependence of the form:

$$\dot{r} = C P^{.51} T_{air}^{.34} G_{air}^{.41} \tag{2}$$

Insufficient runs were made in this investigation at other than ambient
inlet temperature to calculate a temperature dependence for the regression
rate. The above equations for regression rate agree closely for the depen-
dence on G. The dependence on pressure was significantly less in this study.
In the work of Boaz and Netzer, chamber pressure was varied intention-
ally from 37 to 108 psia by varying the throat size. In this study pressure
varied between 33 and 63 psia only as a result of varying combustion effi-
ciency and G. The dependence of regression rate on G results from convective
heat transfer to the fuel surface whereas the dependence on the pressure can
result from radiation and/or finite rate kinetics.

With the application of bypass air, the dependence of regression rate on
pressure and air flux was altered. In Fig. 4 are plotted the 0.2 lbm/sec
non-bypass cases and the bypass runs made with 0.2 lbm/sec total air flow rate
at the nominal test condition. The nominal test condition was a bypass air
flow rate of 0.1 lbm/sec and two dumps with diameters of 2.065 cm. This
corresponded to a dump momentum to fuel grain port momentum ratio of approxi-
mately 0.5. A slightly stronger dependence on pressure was shown while

14

regression rate indicated very little or no dependence on air flux for the
values tested. Here regression rate took the form:

$$\dot{r} = 0.00116P^{.42}G_{air}^{.003} \tag{3}$$

In the bypass situation, the mass flux through the grain is low but the
pressure is maintained high due to the total mass flux through the nozzle
throat. However, correcting the regression rate for the increased pressure
per equation (2) does not result in regression rates as high as the experi-
mental data. In addition, regression rates based on weight and diameter
agreed, indicating that the change did not result from different combustion
behavior within the aft mixing chamber. These conditions of low G and high
P minimize the convective heat flux. At lower G the regression rate
increases relative to the air flux, i.e., more unburned fuel exists under-
neath the diffusion flame within the thicker boundary layer; thus more gas
with radiative properties is present.

(b) Combustion Efficiency

In Fig. 5 are plotted the cases from both Figs. 3 and 4. As can be
seen from this figure the use of bypass air flow in a solid fuel ramjet using
polymethylmethacrylate as a fuel has the effect of reducing combustion
efficiency. For the non-bypass runs, a decrease in air flow also causes a
slight decrease in combustion efficiency. While maintaining the same air
flux through the grain, injecting bypass air into the mixing section brings
a further decrease in performance. Decreasing air flux through the fuel
grain while maintaining the same total flow rate in the bypass case also
brings about a reduction in combustion efficiency. Decreasing the air flux
through the fuel grain increases the percentage of fuel that must be burned
in the aft mixing chamber. Apparently, the mixing chamber was not of

15

sufficient length and/or the bypass air caused quenching of the mixing chamber combustion.

To further study the decrease in performance found when using bypass, other test conditions were considered. Two runs were made with the dumps located behind the aft mixing chamber reattachment point. There was only a slight decrease in combustion efficiency (81%) over that of identical runs in the forward position (83%).

Three runs were made varying the momentum of the individual dumps from the nominal test condition. Small changes in momentum had no effect. Varying the momentum ratio from 0.3 to 1.0 did not significantly change the efficiency. However, when a significantly large increase in momentum was effected (5.3), the combustion performance showed a noticeable decrease (73%).

Only limited data were taken for other than two bypass dumps at 180 degrees. However, the data showed that with low dump momentum two or four dumps spaced at 90 degrees reduced the combustion efficiency. Four dumps at ninety degrees with high momentum decreased the combustion efficiency slightly.

The last variation in geometry studied was the use of swirl in the bypass dump process. This was accomplished by injecting the bypass air with a tangential velocity component. The solid fuel ramjet motor was also run without fuel grain ignition, both with and without swirl, to determine the effect of the induced vorticity on the effective exit nozzle diameter. Decreasing the effective nozzle diameter would increase the combustion chamber pressure and give false indications of higher efficiency. The swirl was found to not affect the effective throat diameter. Two test firing runs were made with swirl, giving an average combustion efficiency of 86%, the highest performance of any bypass run.

16

Every form of bypass used caused a decrease in combustion efficiency. This indicates that the decrease in performance is due to the effect of the bypass air flow on the kinetics of the combustion process within the aft mixing chamber. Essentially equal decreases in performance were obtained with the dump air injected both behind and in front of the reattachment point. Apparently a significant portion of the total combustion process takes place downstream of the reattachment point in the aft mixing chamber. This agress with the temperature data presented by Schadow[7] for an all-hydrocarbon fuel. In the case of PMM, the light weight unburned hydrocarbons that enter the aft mixing chamber apparently burn most completely when allowed to react slowly with the available oxygen in the hot flow from the core of the fuel grain.

The possibility of the temperature of the air entering the aft mixer causing reduced combustion efficiency was considered. A run was made in which the temperature entering both the grain and aft mixer was increased from approximately 292°K (520°R) to 389°K (750°R). The combustion efficiency did not change significantly, indicating that for PMM-air combustion the dump air temperature is probably not as important as the quantity and temperature of the unburned fuel and the mixing rate.

In the region in front of the reattachment point, the less that was done to disturb the flow resulted in better performance. In the case of swirl where the bypass flow remained close to the wall, bypass efficiency was maximized. When the bypass momentum was increased to where the flow disturbed the fuel rich layer between the recirculation region and the air rich central core, performance decreased. This again indicates that a major portion of the combustion process takes place along this fuel rich layer or that the process downstream is highly dependent on the high temperatures in this layer. It

17

also indicates that the combustion mechanisms around this layer are more important than those which occur within the recirculation region. These results imply that different optimum bypass dump configurations and momentum should be expected for different fuel systems.

It is known that the use of bypass improves performance in solid fuel ramjets using all-hydrocarbon fuels. In the case of oxygen-containing fuels and for fuels which decompose into monomers or small hydrocarbon molecules (such as PMM), results indicate that the fuel burns most efficiently without bypass.

The use of bypass systems has meant an increase in weight, cost and complexity of the solid fuel ramjet. In addition, they may introduce combustor-feed system coupling. The use of a fuel which has sufficient density impulse, regression rate and flammability limits to minimize inlet total pressure losses has led to the use of all-hydrocarbon fuels. Although PMM does not meet the criteria for a good fuel, the results of this study indicate that future fuel studies may be fruitful if directed toward ones which contain low percentages of oxidizer and/or substances which unzip the hydrocarbon chain.

(c) Combustion Pressure Oscillations

In the non-bypass test runs, the inlet and combustion pressures exhibited a steady, small amplitude (approximately 2% of chamber pressure) oscillation of approximately 150 Hz. In the bypass runs at nominal conditions, the same oscillation appeared though of considerably higher amplitude (approximately 30% of chamber pressure).

In the case of low or very high aft dump momentum, a second oscillation appeared along with that previously mentioned. This oscillation was of very low frequency (1 Hz.) and large amplitude (approximately 20% of chamber pressure) and may be connected with behavior within the mixing chamber recirculation

18

zone. The bypass-generated very low frequency pressure oscillations are in the range of frequencies which could be coupled to the fuel regression rate. Other fuel/feed systems may exhibit similar or different oscillatory behaviors depending upon the feed system design and the kinetics of the combustion process in the aft mixing chamber.

C. Conclusions and Current Work

The use of bypass air flow in a solid fuel ramjet which utilizes PMM as the fuel decreases the combustion efficiency. Air flow injected into the aft mixing chamber has a more pronounced effect on the combustion process when a high enough momentum is provided for the bypass air to reach the fuel rich shear layer trailing from the port of the fuel grain.

A significant amount of combustion occurs downstream of the reattachment point in the aft mixing chamber. Bypass air injected into the aft mixing chamber also has an effect on the regression rate upstream in the fuel grain. For PMM fuel burned at high pressures and low air mass flux, the principal mechanism for wall heat flux became radiation, and resulted in the regression rate becoming insensitive to the air flux through the fuel port.

With the use of bypass systems it is possible to set up combustor-feed system type oscillations and instabilities dependent upon the effects of the bypass flow on the aft mixing chamber combustion process and on the fuel regression rate.

Current experimental work is being directed at the effects of bypass on the combustion behavior of all-hydrocarbon fuels. In addition, the effects of design and test conditions on combustion pressure oscillations are being investigated.

IV. ANALYTICAL INVESTIGATION

A. Model Overview

The basic assumptions were that the flow was steady, recirculating, two-dimensional and subsonic. In addition kinetic heating and vorticity sources resulting from spatial gradients in the effective viscosity were neglected. The turbulent Lewis number was taken to be unity. The transformed variables of vorticity (ω/r) and stream function (Ψ) were used together with enthalpy (h), and species mass fractions (oxidizer, fuel, etc.). A modified Jones-Launder[6,9,10] two equation turbulence model was used to calculate the viscosity throughout the flow field. Thus, two additional variables must be considered, the turbulence kinetic energy (k) and the turbulence energy dissipation rate (ε). The modified Jones-Launder model incorporates five empirical constants and the effective viscosity is calculated using the following expression:

$$\mu_{eff} = 0.09\rho k^2/\varepsilon \tag{4}$$

In the present study the combustion was considered to be mixing limited with a one-step simple chemical reaction. Thus, 1 gm fuel + i gm oxidizer → (1+i) gm of products and fuel and oxidizer could not exist together. Species considered were oxygen, nitrogen, fuel and products. The present form of the model neglected radiation and density was calculated using $\rho = p\bar{M}/RT$.

With these assumptions the governing equations for axisymmetric flow can be cast in the standard elliptic format[5,6,9]

$$a_\phi \left[\frac{\partial}{\partial z}\left(\phi \frac{\partial \Psi}{\partial r}\right) - \frac{\partial}{\partial r}\left(\phi \frac{\partial \Psi}{\partial z}\right)\right] - \underbrace{\frac{\partial}{\partial z}\left[b_\phi r \frac{\partial(C_\phi \phi)}{\partial z}\right] - \frac{\partial}{\partial r}\left[b_\phi r \frac{(C_\phi \phi)}{\partial r}\right]}_{\text{diffusion terms}} + \underbrace{r S_\phi}_{\text{source term}} = 0 \tag{5}$$

$$\underbrace{\phantom{a_\phi \left[\frac{\partial}{\partial z}\right]}}_{\substack{\text{convection} \\ \text{terms}}}$$

20

where the parameters are presented in Table II. Additional discussion of these equations and utilization of various turbulence models can be found in Ref. 11 and 12.

Table II. Equation Parameters[5,6]

ϕ	a_ϕ	b_ϕ	C_ϕ	S_ϕ
$\dfrac{\omega}{r}$	r^2	r^2	μ_{eff}	$-\dfrac{\partial}{\partial z}(\rho v_\theta^2) - r[\dfrac{\partial}{\partial z}(\dfrac{v_r^2 + v_z^2}{2})\dfrac{\partial \rho}{\partial r} - \dfrac{\partial}{\partial r}(\dfrac{v_r^2 + v_z^2}{2})\dfrac{\partial \rho}{\partial z}]$ $- r^2 S_\omega$
ψ	0	$\dfrac{1}{\rho r^2}$	1	$-\dfrac{\omega}{r}$
$m_{fu} - \dfrac{m_{ox}}{1}$	1	$\dfrac{\mu_{eff}}{\sigma_{of}}$	1	0
m_{N_2}	1	$\dfrac{\mu_{eff}}{\sigma_{N_2}}$	1	0
h	1	$\dfrac{\mu_{eff}}{\sigma_h}$	1	0
k	1	$\dfrac{\mu_{eff}}{\sigma_k}$	1	$-(G - \rho\varepsilon)$
ε	1	$\dfrac{\mu_{eff}}{\sigma_\varepsilon}$	1	$-(C_1 G\varepsilon/k - C_2 \rho\varepsilon^2/k)$

$$C_1 = 1.45 \, , \; C_2 = 2.0 \, , \; V_\theta = 0$$

$$S_\omega = S_\omega \; (\text{gradients in } \mu_{eff}) \rightarrow \text{neglected}^{5,12}$$

$$\sigma_h = \sigma_{of} = \sigma_{N_2} = \sigma_k = 1.0, \; \sigma_\varepsilon = 1.3$$

B. Boundary Conditions And Solution Procedure

The inlet flow was considered to be "plug flow" although other inlet conditions (distortion, etc.) are easily incorporated. The inlet turbulence intensity was taken to be 5.2% in order to closely match experimental measurements. Axial gradients for all variables were considered zero at the flow exit and were taken as zero for all "conserved properties" $(m_{fu} - \frac{m_{ox}}{i}, m_{N_2}, h)$ at the step-face. Radial gradients for all variables except Ψ were taken as zero at the axis of symmetry. The major area of concern in the specification of boundary conditions for the SFRJ is along the fuel surface. When calculations are made with the model for an adiabatic or isothermal wall with no mass addition, inaccuracies in the turbulence model are somewhat masked. The fuel mass addition at the wall and the subsequent combustion greatly amplify the need for accurate effective viscosity calculations near the wall if observed experimental behavior is to be approximated.

All "conserved" properties when in dimensionless form, had identical governing equations and boundary conditions. Thus, only one equation was required to be solved for all "conserved" properties. The resulting set of five equations $(\frac{\omega}{r}, \psi, k, \varepsilon, m_{fu} - m_{ox}/i)$ were cast in finite difference form and solved using the Gauss-Seidel method with upwind differences and relaxation. Under relaxation was required: 0.5 for $\frac{\omega}{r}$ and ψ, 0.3 for k and ε, and 0.9 for $m_{fu} - m_{ox}/i$. A non-uniformily spaced 17 x 25 rectangular grid system was employed. Solution was performed on an IBM 360-67 using Fortran H and required approximately thirty-five minutes to complete 1000 iterations.

The fuel surface was considered to have a uniform and constant temperature and the mass fraction of oxidizer at the surface was considered to be zero. In order to obtain a fuel rich recirculation zone, a boundary layer flame

pattern in agreement with experiment, and accurate conservation of species, several modifications had to be made to the original model[6,10]. For simplicity the boundary layer was considered to consist of two parts, a laminar sublayer and a turbulent layer. The border between the two regions was considered to occur where $y_p^+ = 24$. At each near wall grid point y_p^+ was calculated.

$$\text{If } y_p^+ > 24: \quad C_{fo}/2 = 0.02846/R_e^{0.25} \tag{6}$$

The velocity profile was corrected for blowing[13] and μ_{eff} was calculated using Eq. (4).

$$\text{If } y_p^+ \leq 24: \quad C_{fo}/2 = 2/R_e \ . \tag{7}$$

The laminar viscosity was calculated using

$$\mu = \mu_o \ (T/T_o)^{0.5} \tag{8}$$

In the actual calculation procedure, the grid was selected to insure that $y_p^+ \leq 24$. The value of 0.02846 is required for matching of the two-zone boundary layer.

The boundary condition for vorticity was calculated from

$$\left(\frac{\omega}{r}\right)_o = \frac{\tau_o}{\mu_o \ r_w} \quad \text{where} \quad \tau_o = (C_{fo}/2) \ \overline{\rho v} \ \ln (1 + B)/B \tag{9}$$

in which the wall shear stress is corrected for blowing by using the simple Couette flow approximation $\ln(1 + B)/B$. The control volumes used at the fuel surface for the micro-integration are shown in Fig. 6. The control volume for all variables but k and ε were taken to the wall. For k and ε the control volumes were taken to the half-grid point. Gradients at the wall for "conserved" properties were taken to be of the form

23

$$\left(\frac{\partial h}{\partial y}\right)_o = \{(h_p - h_o)/y_p\} \ln(1 + B)/B \tag{10}$$

The wall mass flux provided the boundary condition for Ψ and was calculated from

$$\dot{m}'' = \left(\frac{\mu_o}{P_r}\right)\left(\frac{\partial h}{\partial y}\right)_o/(h_o - h_T) = \left(\frac{\mu_o}{P_r}\right)\frac{\ln(1+B)}{y_p} \tag{11}$$

The boundary condition on k was calculated from[6]

$$k_o = \gamma k_p \tag{12}$$

$$\gamma = -1.0, \quad R_t \le 19.8$$

$$= -0.39, \quad R_t > 19.8$$

The boundary condition on ε was considered to occur at the near wall grid point

$$\varepsilon_p = k_p^{3/2}/\ell_p \tag{13}$$

where

$$\ell_p = 0.2 \, y_p, \quad y_p^+ < 24 \tag{14}$$

$$\ell_p = 0.4 \, y_p, \quad y_p^+ > 24 \tag{15}$$

The boundary conditions for $\frac{\omega}{r}$, k and ε on the step face were calculated in a similar manner except that there was no wall mass addition, none of the micro-integration control volumes were extended to the wall, and $\ell_p = 2.44 \, y_p$.

Launder and Spalding[14] have discussed the strengths and weaknesses of the k-ε model using both the wall function and low-Reynolds-number modeling methods. They indicate that modification of the boundary conditions on ε were sometimes found necessary on the step face in order to obtain results in agreement with experiment. In this investigation wall-functions were employed

24

for the k-ε model. Since the mass addition rates were low ($B < 1.5$) the five constants in the model[6,9,10] were not modified. When $y_p^+ < 24$ along the fuel grain the effective viscosities predicted using the k-ε model were not used at the near wall grid points. In this case, the boundary conditions given by Eqns. (13), (14) and (15) were required to provide realistic values of μ_{eff} and fuel mass fraction at the second grid point from the wall. An alternate procedure could have been to use the low-Reynolds-number modeling methods[10,14]. In recent work with smaller inlet step heights it has been found necessary to employ Eqns. (13), (14), and (15) for ε_p along the step face. Much additional work is apparently required to better define the near-wall region.

The finite-difference equations[5,6] require the use of space averaged values for the source terms presented in Table II. At the near wall grid points large gradients exist if $y_p^+ > 24$. As mentioned above, this was prevented at the fuel surface by appropriate selection of the radial grid spacing. Along the step face, however, integrated average values had to be calculated for $\frac{\omega}{r}$ and all velocity gradients. Velocity profiles along the step face for $y_p^+ > 24$ were assumed to obey the 1/7th power law.

In order to obtain realistic solutions the stream function at the grid point downstream of the step inlet was required to be held fixed at the value which existed at the step corner.

C. Results and Discussion

Divergence would occur in the iteration unless the initial conditions specified for ω/r and ψ were in close agreement (for example, 1/7th power law distributions). It was also necessary to prescribe an initial length scale distribution. The length scale distribution was used to calculate initial values of ε from k using Eqn (13). The ε field was

held constant for an initial 35 iterations in order to promote convergence. Specification of the initial length scale distribution required trial and and error methods for other than the simple rearward facing step geometry. Variations in gas density were also prevented from varying for the first 50 iterations.

At each axial location species and energy conservation calculations were made. False diffusion errors were larger in the recirculation zone where the grid lines were at large angles to the streamlines. Small errors in the solution of the "conserved" property equation presented some difficulties since m_{fu}, m_{ox}, m_{pr} and m_{N_2} were all calculated from the one solution. Calculation of fuel conservation was especially difficult since fuel concentration gradients near the wall were very large. In general, energy and species (other than fuel) were conserved to within five percent. With these accuracies, fractional changes between iterations were a maximum of 0.3 percent. This required between 750 and 1000 iterations. The "conserved" properties and stream function converged more rapidly than did $\frac{\omega}{r}$, k and ε, For the higher inlet velocities, the relaxation parameter for $\frac{\omega}{r}$ had to be reduced to values between 0.3 and 0.4.

The location of the "reattachment point" was found to be somewhat sensitive to the distance from the step face to the first axial grid line This resulted from specification of the stream function as unchanging as discussed above. However, once a particular grid was chosen which yielded a reattachment point in agreement with experiment for one step height and inlet velocity, good results were obtained for other step heights and inlet conditions. The reattachment point was found to be insensitive to inlet velocity and was found to move slightly upstream with low rates of wall mass addition. Both of these results are in good agreement with experimental data[8,15].

26

A true reattachment point does not exist when mass addition through the wall is present. However, a pseudo-reattachment point was calculated by assuming it to occur where the average velocity was zero between the wall and the near-wall node. A comparison of this "reattachment point" with chemical reaction is made with experimental data from non-reacting flows in Fig. 7. It should be noted that the predicted flow reattachment occurred downstream of the Krall-Sparrow[16] maximum heat transfer point but upstream of the Phaneuf-Netzer[15] data with 10% wall mass addition.

Typical predicted streamline patterns and temperature distributions are presented in Figure 8 for plexiglas fuel and air. The dividing stream-line is also sketched in the temperature field. The recirculation region was calculated to be fuel rich and the flame initiated along the shear layer and spread out as it approached the reattachment region. The flame region was located within the developing turbulent boundary layer downstream of the reattachment zone. These observations are in qualitative agreement with experiment.

A comparison of predicted plexiglas fuel regression rates with experiment is presented in Figure 9. It should be noted that the location of the maximum regression rate obtained experimentally was affected by the inlet air distortion/turbulence intensity. The model predicts a maximum regression rate upstream of the experimental values and slightly upstream of the Krall-Sparrow[16] location for maximum heat transfer in non-reacting flow. The average fuel regression rate was in good agreement with experiment and the regression pattern was qualitatively correct (although shifted upstream). In the present model only convective transfer to the fuel surface is considered. The predicted regression profile may not be correct for fuel systems which produce large amounts of radiative heat transfer to the surface.

27

Figure 10 compares the predicted centerline turbulence intensity (assuming isotropic turbulence) with experimental data for non-reacting flow The behavior with axial distance was generally in good agreement but the inlet region exhibited behavior not observed experimentally. The model overestimates the velocity increase of the air as it enters the combustor, which in turn reduces the predicted turbulence intensity.

Figure 11 compares experimental and predicted axial pressure profiles. The experiment and theory were not for identical conditions, but in general it is seen that the model predicts the pressure to level-off upstream from experimental measurements. This was expected since the model underestimated the distance to the reattachment point. Pressure calculations were very sensitive to solution accuracy since they depend upon second derivatives of stream-function.

Figure 12 presents predicted radial temperature profiles as a function of inlet step size and air flow rate at a location downstream of flow reattachment. As the air flow rate was reduced for a fixed step size, the peak temperature moved further from the wall, the core flow became hotter, and the overall fuel-air ratio increased. This results from the fact that regression rate varies as the 0.3 to 0.5 power of G_{air}. Actually the model predicted that $\dot{r} \sim G_{air}^{0.3}$, whereas experimentally it was found for plexiglas that $\dot{r} \sim G_{air}^{0.4}$.

The recirculation zone in the solid fuel ramjet acts as the flame stabilization device. It operates fuel rich but, when operating within certain limits, provides enough energy to heat the air in the shear layer to the point where the downstream boundary layer flame can be stabilized in the high velocity flow. As the inlet flow rate was increased the temperature in the upstream portion of the recirculation zone was found to increase. This resulted from the increased air flux into the fuel rich portion of the

zone. However, this same increased air flux into the recirculation zone decreased the temperature in the downstream portion of the zone and at the reattachment position. Thus, although the peak temperatures in the recirculation zone increased with increased inlet air velocity, the oxygen reaching the downstream flame zone decreased in temperature. In addition, the boundary layer flame narrows and moves closer to the wall. Eventually a condition would be reached where the oxygen reaching the boundary layer flame region would be too low in temperature to sustain the narrowed flame which exists in the relatively high velocity region close to the fuel surface. Earlier work with the model[1,4], in which one-step finite rate kinetics where employed, also demonstrated that increased inlet velocity can cause flame blow-off in either the recirculation region or the boundary layer region.

Decreasing the inlet step size decreased the length of the shear layer (reattachment occurred further upstream) and decreased the air entrainment into the recirculation region. Although the shear layer was shorter in length, contact time with the recirculation zone did not necessarily decrease because the inlet velocity was lower. However, the model predictions showed a decreased temperature in the recirculation zone, resulting from a still more fuel rich mixture, and lower temperatures near reattachment. Again it would be expected that a flammability limit would be reached with increasing inlet diameter.

Figure 13 presents the calculated percentage of unburned fuel as a function of air flow rate. As discussed above, the fuel mass fraction was the least accurate calculation. Thus, the results can only be interpreted qualitative. As G_{air} is decreased, an increasing amount of unreacted and hotter fuel is passed into the aft mixing region downstream from the end of the fuel grain.

29

Schadow[7] has made measurements of temperature and species concentrations in a reacting solid fuel ramjet. His experiments utilized an all-hydrocarbon fuel which results in significant radiative heat transfer to the fuel surface and higher fuel regression rates. However, the data are all that is currently available for SFRJ model validation in the reacting flow environment. Because the regression rate predicted using only convective heat transfer was too low for the radiative system, the predicted regression rates along the length of the fuel grain were arbitrarily increased by 30%. This cannot be expected to yield the correct axial variations in regression rate but was done to obtain a more realistic value of the blowing parameter for the higher regression rate system.

Figs. 14, 15, and 16 present the theoretical temperature profiles compared to the data of Schadow[7] for different air mass fluxes and axial locations within the fuel grain. The theoretical temperature profiles are not for exactly the same L_p/D_p locations as the experimental data. The profiles at the nearest corresponding grid line have been presented.

Fig. 14 presents data for the high mass flux condition. The model predicts more complete mixing and therefore more uniform temperatures in the recirculation zone (L_p/D_p = 0.52) than the data. In the region near reattachment (L_p/D_p = 2.3) the experimental data indicates an apparent "two-flame" zone. It is possible that just upstream of reattachment one flame may exist very close to the wall and another could result, farther from the wall, from the recirculating, reacting shear layer. However, the data of Schadow has not been corrected for radiation effects and an L_p/D_p of approximately 2.0 should be the most downstream location of reattachment for the inlet step height employed. If this "two-flame" region is characteristic of the flow near reattachment, then the model fails to predict this detail. There could be

several reasons for this possible weakness in the model. Radiation is neglected in a system which produces large amounts of radiation. In addition the $K-\epsilon$ model and/or the boundary conditions specified on the fuel surface for shear stress could result in a "smearing-out" of the species distributions in the radial direction near the wall where large property gradients exist. Downstream of reattachment where the boundary layer develops $(L_p/D_p = 5.2, 6.1)$ the profiles are in better agreement with experiment. The centerline temperature increase with axial distance is reasonably predicted.

Similar results for lower air fluxes can be observed in Figs. 15 and 16. The model, without radiation-convection coupling to determine the fuel regression rate, predicted a stronger dependence of regression rate on air flux than obtained experimentally. This will also affect the predicted temperature profiles. The model does correctly predict the increasing boundary layer thickness with resulting peak temperatures further from the wall and higher centerline temperatures as the air flux is decreased. The regression rate variation with axial distance is different for the all-hydrocarbon system than for the convection dominated PMM fuel system. The model does a reasonable job of predicting this profile for PMM. For both fuels the regression rate increases from the head-end to near the reattachment zone and then decreases. Further downstream the PMM regression rates (and the model predictions) continue to decrease and/or level off whereas the all-hydrocarbon regression rates begin to increase again.

The model assumed mixing limited and complete combustion so that "products" consisted only of H_2O and CO_2. This is obviously an oversimplification but perhaps warranted when compared to the other simplifications employed in the model. Schadow[7] has measured with a probe the radial variation in moles of free O_2 per mole of N_2 at the exit plane of the fuel

31

grain. A comparison of his data with the model is presented in Fig. 17. Schadow[7] found that in order to predict the correct variation in combustion temperature with mixture ratio in the fuel port, 40% of the carbon present had to be assumed as unreactive soot particles. As a qualitative attempt to compare the model (with infinite rate kinetics and no free carbon) with the data of Schadow, 40% of the carbon in "CO_2 products" was assumed unreactive. The oxygen from the CO_2 was combined with the unreacted O_2 to produce a new profile for the moles of "free" O_2. The results are presented in Fig. 17. and show reasonable agreement with experiment.

D. Conclusions and Current Work

Temperature, pressure, turbulence intensity, and species profiles as well as the flow reattachment position were in qualitative agreement with experiment. The largest discrepancies existed in the recirculation region and near the fuel grain at reattachment. Regression rate profiles were in good agreement except for the all-hydrocarbon fuel far downstream from reattachment. The model appears to be adequate for qualitative evaluation of the effects of geometry and test conditions on the flame pattern and the amount of unburned fuel entering the aft mixing chamber. In order to obtain better quantitative results, radiation and finite rate, multiple-step kinetics should be incorporated into the model. Further work is required to validate the k-ε model, especially in the near-wall regions.

The Ψ-ω variables make it difficult to obtain accurate predictions of the pressure field and to specify boundary conditions on the walls. The point iterative method employed also requires a large storage space and long computation times.

Current work with the model includes (a) extending its application to include the aft-mixing geometry as shown in Fig. 1 and (b) using the primary variables of pressure and velocity in place of the Ψ-ω variables.

V. REFERENCES

1. Jones III, C.E., Phaneuf, J.T., and Netzer, D.W., "An Investigation of the Intenral Ballistics of Solid Fuel Ramjets", 11th JANNAF Combustion Meeting, CPIA 261, Vol II, Dec 1974, pp 449-470.

2. Bulban, E.J., "Light Rocket Features Solid-Fuel Ramjet" Aviation Week, July 31, 1961, pp 87-90.

3. Jensen, G.E., Dunlap, R., Holzman, A.L., "Solid Fuel Ramjet Flame Stabilization and Fuel Regression Studies", 12th JANNAF Combustion Meeting, CPIA No. 273, Vol II, Dec. 1975, pp 425-439.

4. Netzer, D.W., "Modeling Solid Fuel Ramjet Combustion", 12th JANNAF Combustion Meeting, CPIA 273, Vol II, Dec. 1975, pp 441-450.

5. Gosman, A.D., Pun, W.M., Runchal, A.K., Spalding, D.W., and Wolfstein, M., Heat and Mass Transfer in Recirculating Flows, Academic Press, 1969.

6. Spalding, D.B., Gosman, A.D., and Pun, W.M., The Prediction of Two-Dimensional Flows, Short Course, Penn. State Univ., August 1973.

7. Schadow, K.C., Cordes, H.F., and Chieze, D.J., "Experimental Studies of Combustion Processes in Solid Fueled Ramjets", 13th JANNAF Combustion Meeting, CPIA 281, Vol III, December 1976, pp 245-259.

8. Boaz, L.D. and Netzer, D.W., "An Investigation of the Internal Ballistics of Solid Fuel Ramjets", Naval Postgraduate School Report, NPS-57Nt73031A, March, 1973.

9. Launder, B.E. and Spalding, D.B., Lectures in Mathematical Models of Turbulence, Academic Press, 1972.

10. Jones, W.P. and Launder, B.E., "The Prediction of Laminarization with a Two-Equation Model of Turbulence", Int. J. Heat Mass Transfer, Vol. 15, 1972, pp 301-314.

11. Kaul, U.K. and Frost, W., "Turbulent Atmospheric Flow over a Backward Facing Step", NASA CR-2749, Oct. 1976.

12. Anasoulis, R.F. and McDonald, H., "A Study of Combustor Flow Computations and Comparison with Experiment", EPA-650/2-73-045, Dec. 1973.

13. Marxman, G.A. and Gilbert, M., "Turbulent Boundary Layer Combustion in the Hybrid Rocket", Ninth Symposium (Int.) on Combustion, Academic Press, 1963, p 371.

14. Launder, B.E. and Spalding, D.B., "The Numerical Computation of Turbulent Flows", Comp. Meth. in App. Mech. and Eng, 3, 1974, pp 269-289.

15. Phaneuf, Jr., J.T. and Netzer, D.W., "Flow Characteristics in Solid Fuel Ramjets", Naval Postgraduate School Report, NPS-57Nt74081, July 1974.

16. Krall, K.M. and Sparrow, E.M., "Turbulent Heat Transfer in the Separated, Reattached, and Redevelopment Regions of a Circular Tube", J. Heat Transfer, Feb. 1966, p 131.
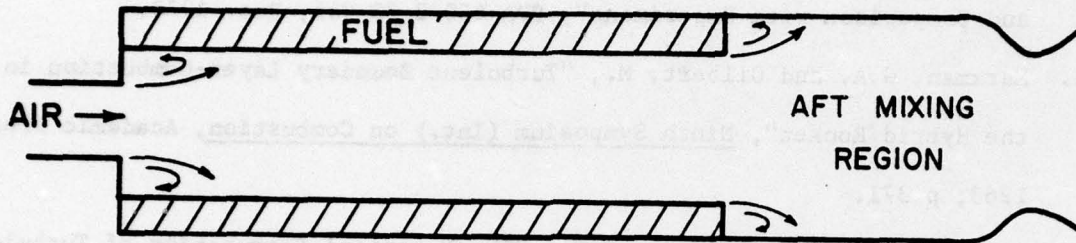
Fig. 1. Schematic of Solid Fuel Ramjet
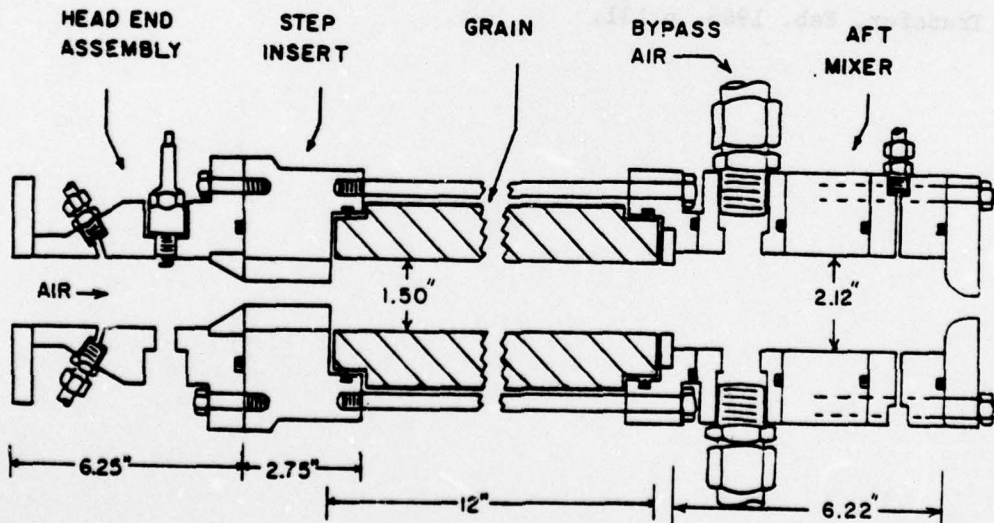
Fig. 2. Schematic of Solid Fuel Ramjet Apparatus
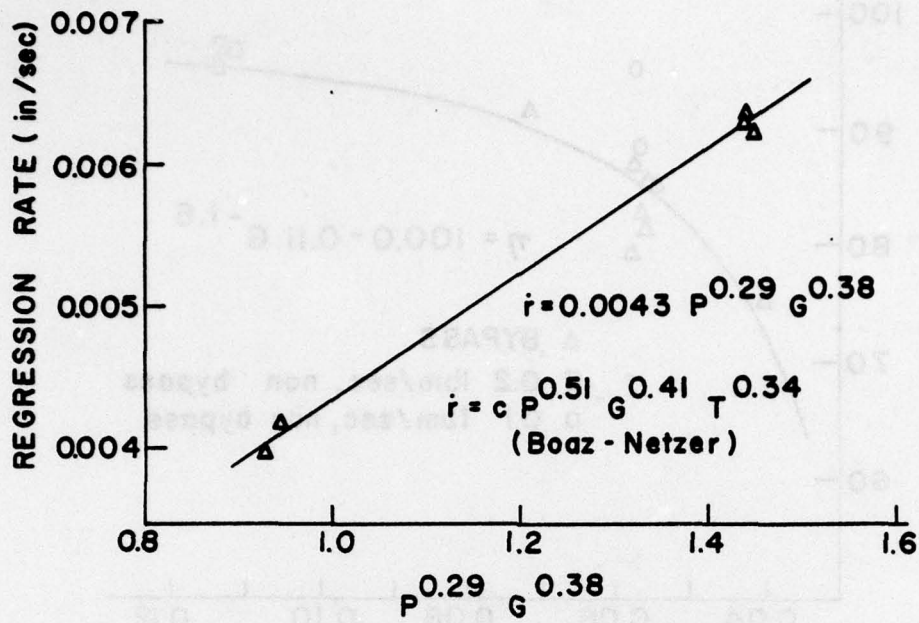
Fig. 3. PMM Regression Rate- Non-Bypass
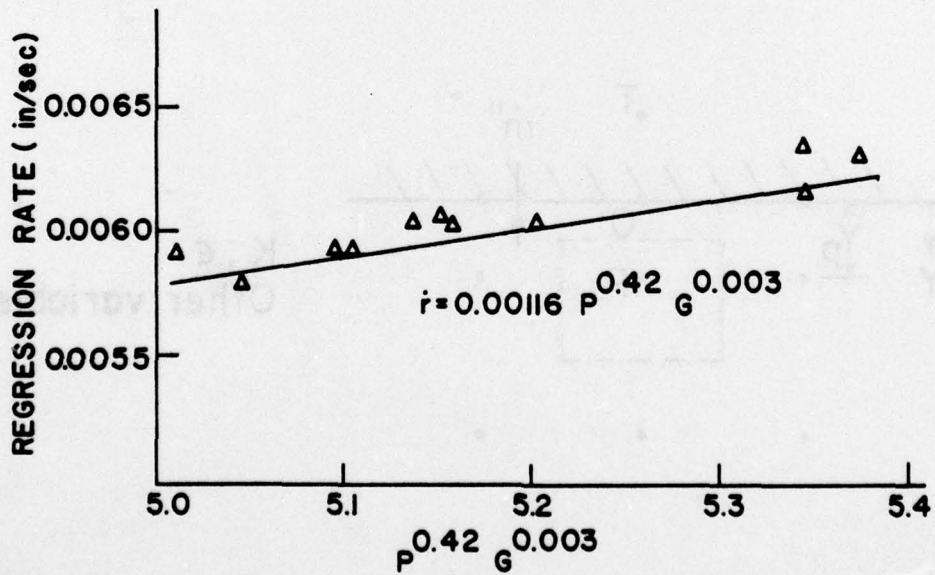
Fig. 4. PMM Regression Rate, Bypass

37
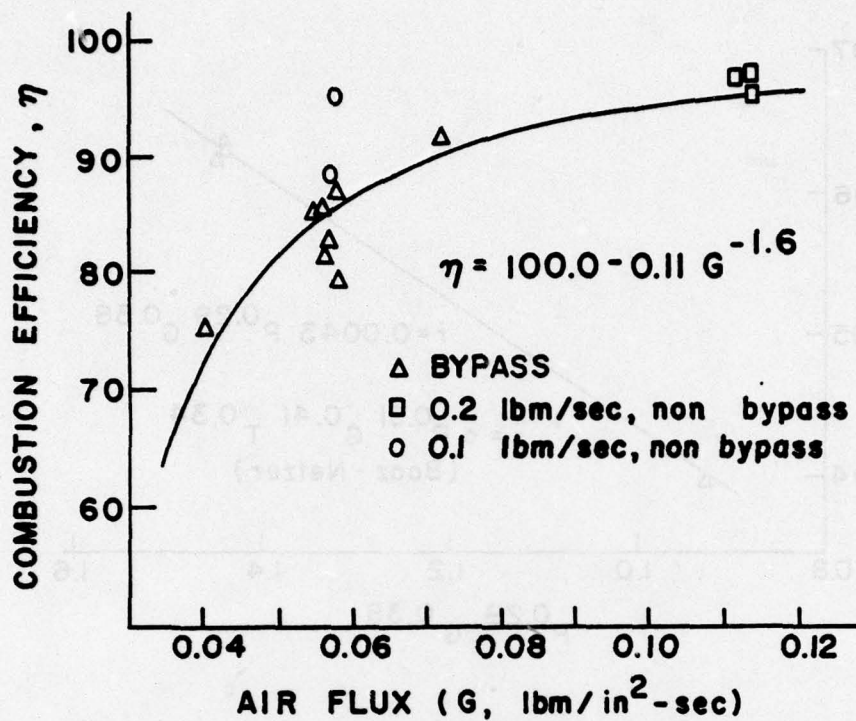
Fig. 5. PMM Combustion Efficiency vs. Air Flux

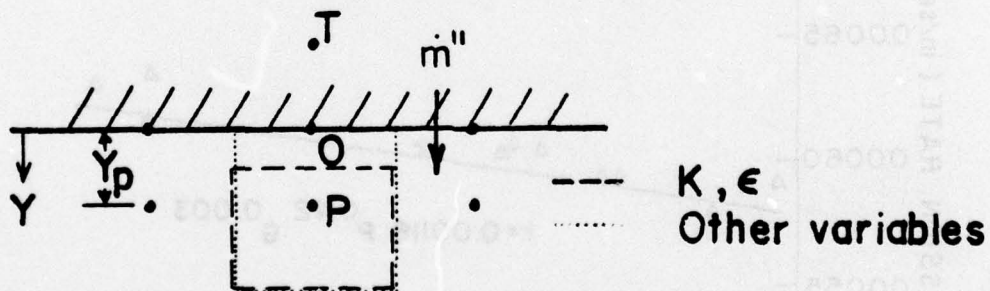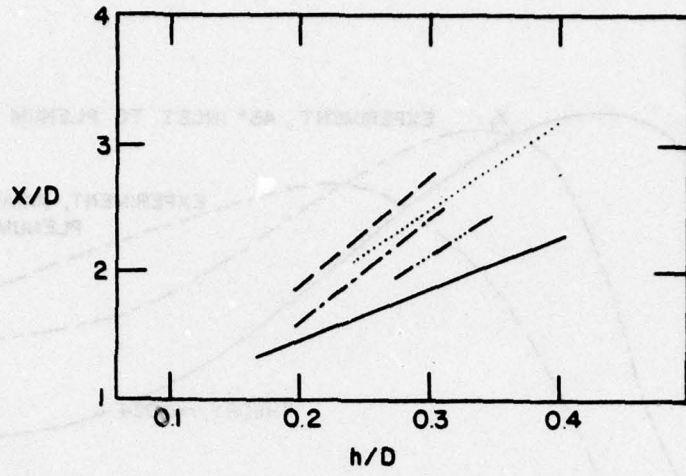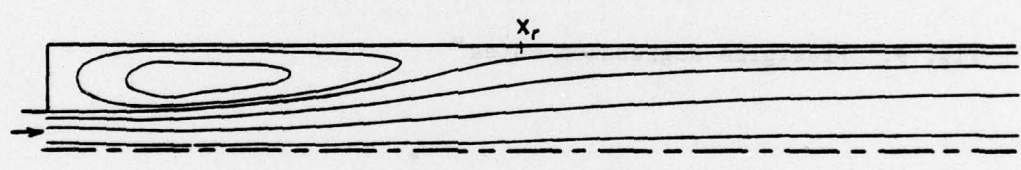$$\eta = 100.0 - 0.11\,G^{-1.6}$$

△ BYPASS
□ 0.2 lbm/sec, non bypass
○ 0.1 lbm/sec, non bypass

Fig. 6. Near-Wall Control Volumes

Fig. 7. Reattachment Locations for Axisymmetric Flows

STREAM-LINE PATTERN
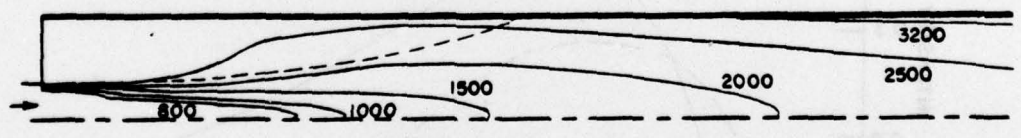
TEMPERATURE DISTRIBUTION , °K

INLET VELOCITY = 197.4 m/sec $\bar{r}$ = 0.024 cm/sec
h/D = 0.321   A/F = 7.36 at L/D = 8.8
X_r/D = 2.31 $(A/F)_{stoic.}$ = 8.231
DIAMETER = 3.81 cm G_{air} = 7.06 gm/cm^2-sec

Fig. 8. Predicted Streamline and Temperature Distributions

39
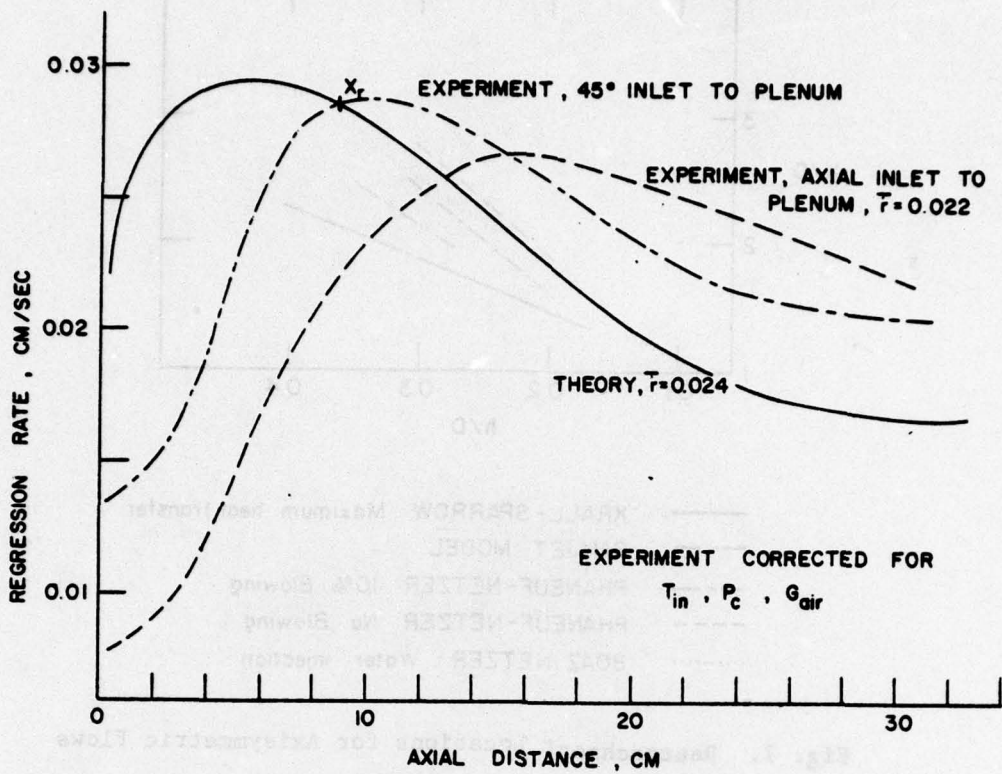
Fig. 9. Plexiglas Regression Rates
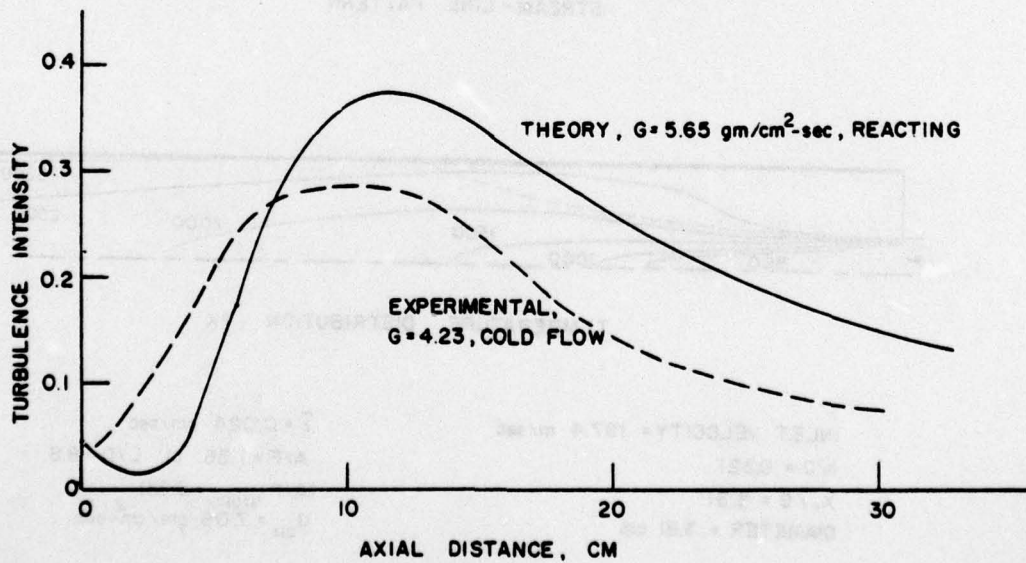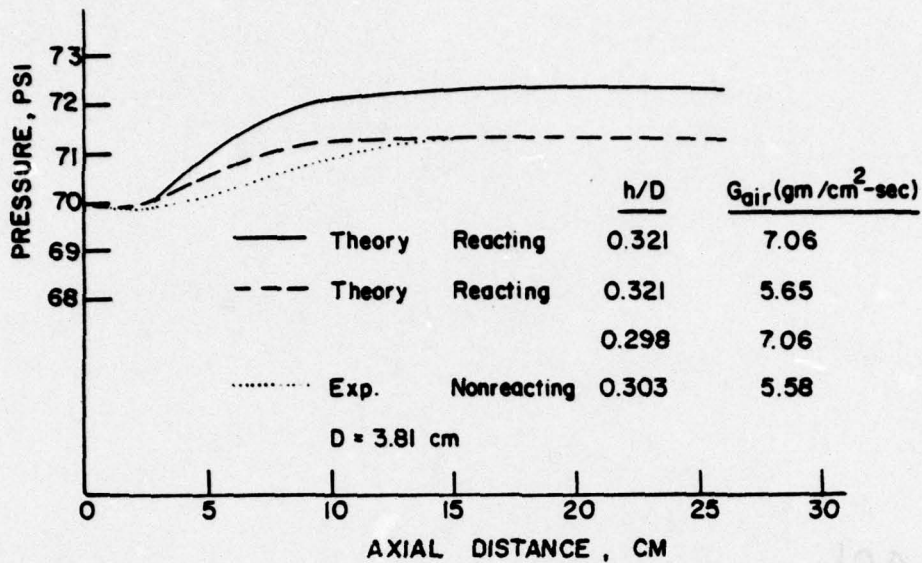

Fig. 10. Centerline Turbulence Intensity

PRESSURE, PSI

73
72
71
70
69
68

		h/D	G_{air}(gm/cm^2-sec)
—— Theory	Reacting	0.321	7.06
——— Theory	Reacting	0.321	5.65
		0.298	7.06
········ Exp.	Nonreacting	0.303	5.58

D = 3.81 cm

0   5   10   15   20   25   30

AXIAL DISTANCE, CM

Fig. 11. Axial Pressure Distributions

RADIAL DISTANCE, CM

2.0   FUEL SURFACE

	h/D	G_{air}(gm/cm^2-sec)
········	0.298	7.06
——	0.321	7.06
———	0.321	6.35
—·—·	0.321	5.65

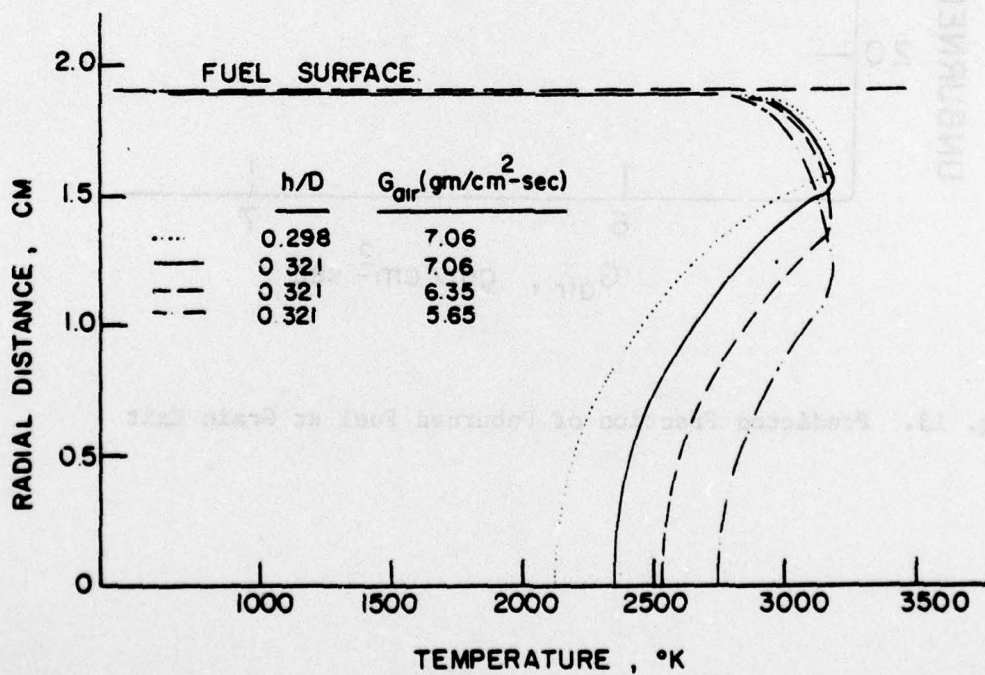1000   1500   2000   2500   3000   3500

TEMPERATURE, °K
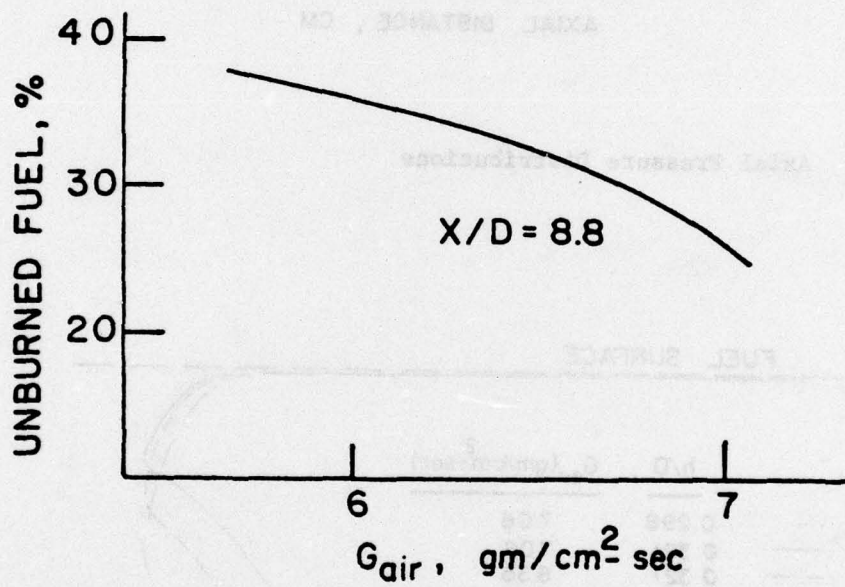
Fig. 12. Predicted Radial Temperature Distributions

41

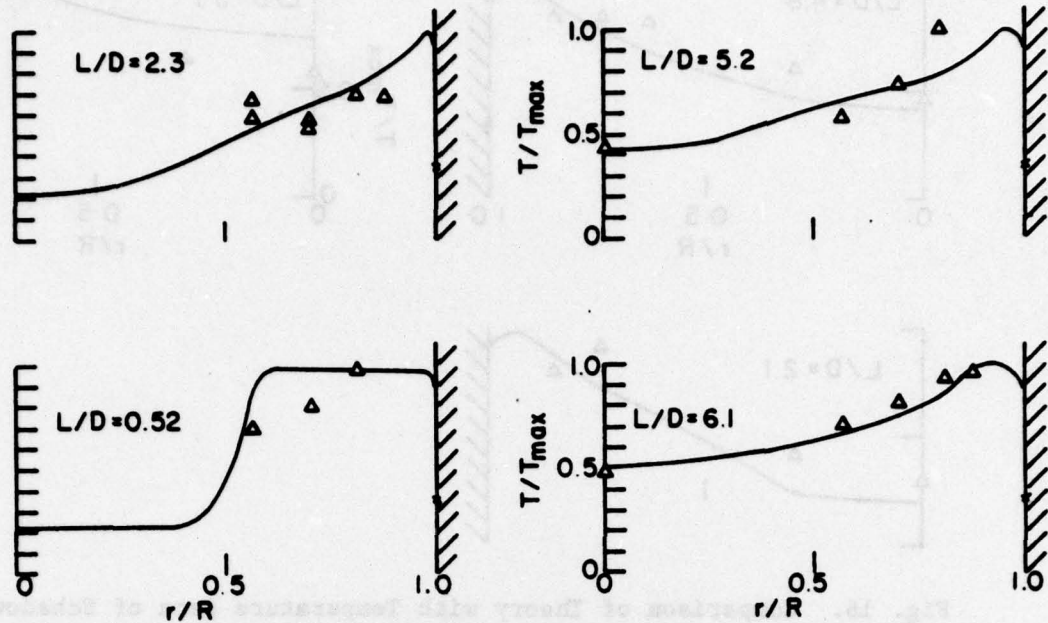Fig. 13. Predicted Fraction of Unburned Fuel at Grain Exit

Fig. 14. Comparison of Theory with Temperature Data of Schadow (G_{air} = 34.5 gm/cm^2-sec (0.49 lbm/in^2-sec), P_c = 8.47 atm, D_p = 7.11 cm, L_p = 50.8 cm, T_{air} = 605°K, A_p/A_i^c = 2.74)
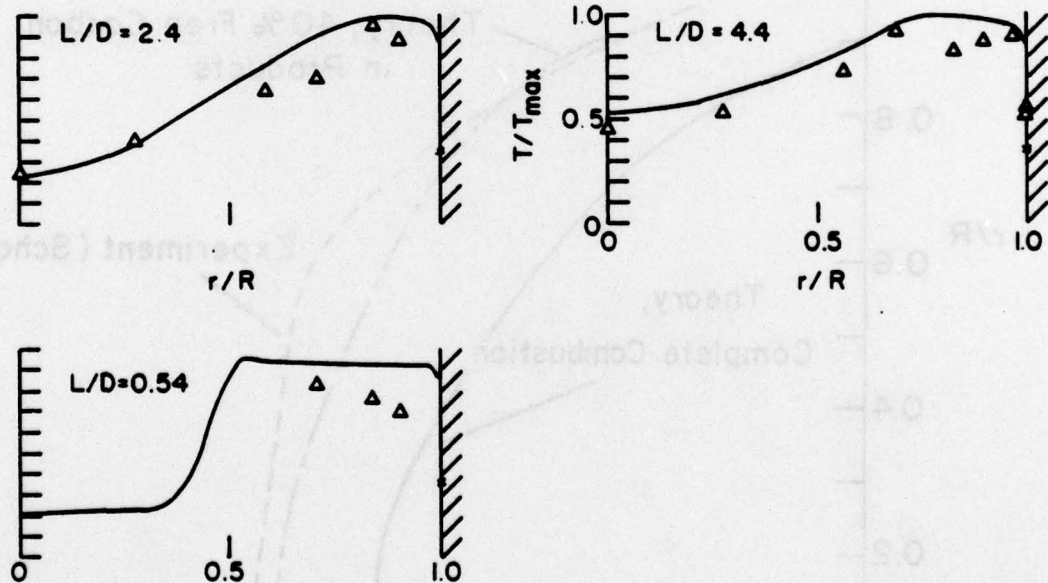

Fig. 15. Comparison of Theory with Temperature Data of Schadow (G_{air} = 16.2 gm/cm^2-sec (0.23 lbm/in^2-sec), P_c = 6.73 atm, D_p = 7.11 cm, L_p = 35.6 cm, T_{air} = 590°K, A_p/A_i = 3.55)
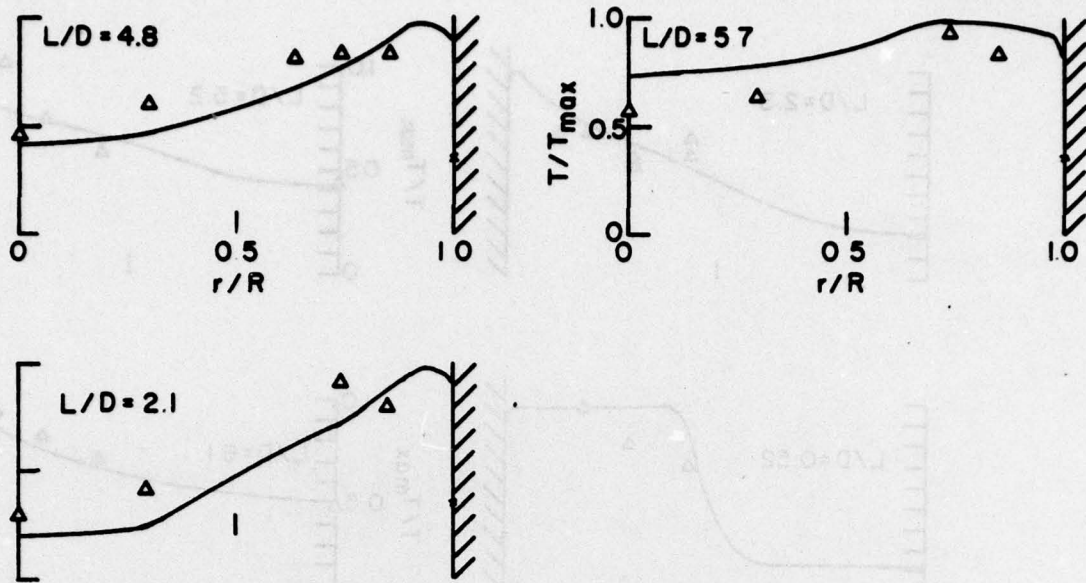
43

Fig. 16. Comparison of Theory with Temperature Data of Schadow (G_{air} = 13.4 gm/cm^2 - sec (0.19 lbm/in^2 - sec), P_c = 6.8 atm, D_p = 7.11 cm, L_p = 50.8 cm, T_{air} = 550°K, A_p/A_i = 3.20)
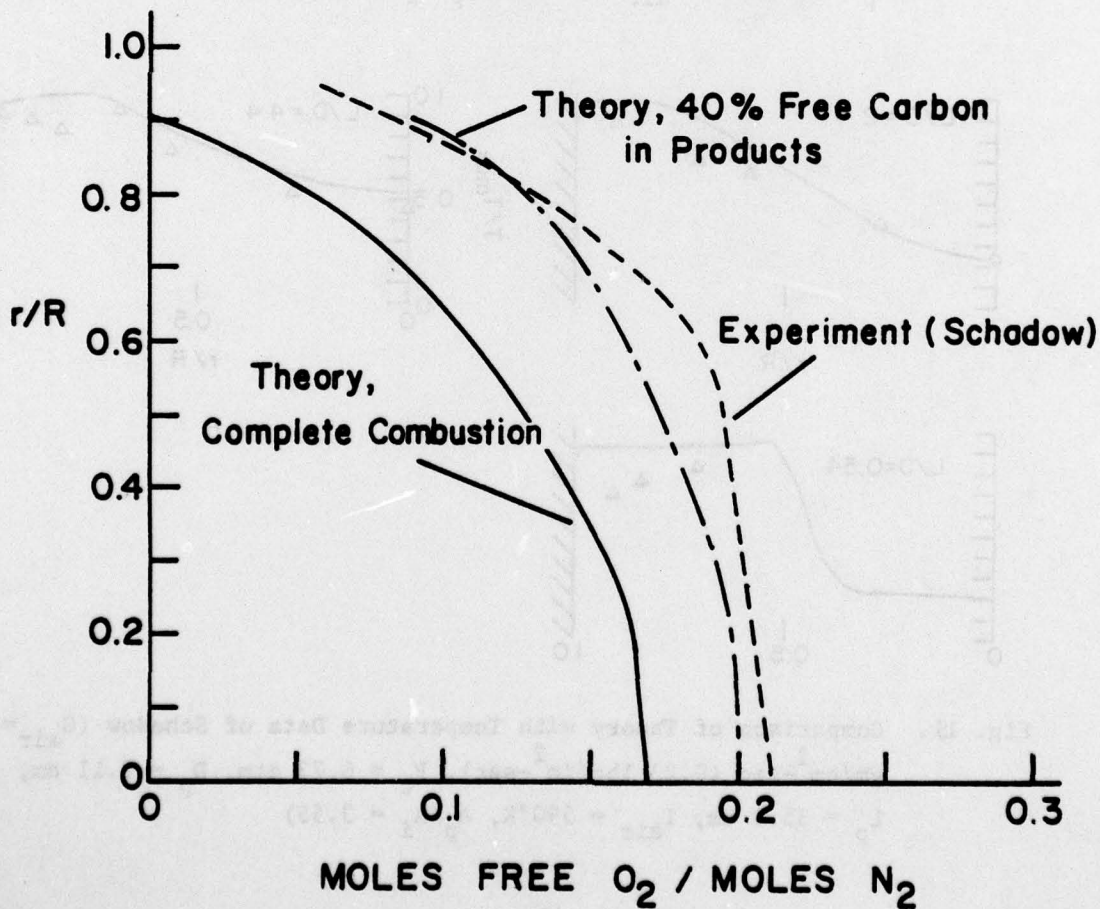

Fig. 17. Comparison of Theory with Concentration Data of Schadow

44

INITIAL DISTRIBUTION LIST

		No. of Copies
1.	Library, Code 0212	2
	Dean of Research, Code 012	2
	Naval Postgraduate School	
	Monterey, CA 93940	
2.	Department of Aeronautics	
	Code 67	
	Naval Postgraduate School	
	Monterey, CA 93940	
	Prof. R. W. Bell, Chairman	1
	Prof. D. W. Netzer,	10
	P. J. Hickey	2
3.	Defense Documentation Center	2
	Attn: DDC-TCA	
	Cameron Station, Bldg. 5	
	Alexandria, VA 22314	
4.	Naval Air Systems Command	
	Washington, DC 20361	
	AIR-330	2
	AIR-536 (Attn: LT J. Mady)	3
5.	Naval Weapons Center	
	China Lake, CA 93955	
	Tech. Library, Code 753	3
	F. Zarlingo, Code 3246	3
	K. Schadow, Code 388	1
.	Chemical Systems Division	
	United Technologies	
	P. O. Box 358	
	Sunnyvale, CA 94088	
	Tech. Library	1
	R. Dunlap	1
	A. Holzman	1
	G. Jensen	1
	P. Willoughby	1
	P. LaForce	1
.	Chemical Propulsion Information Agency	2
	APL-JHU	
	Johns Hopkins Road	
	Laurel, MD 20810	
8.	AFAPL	
	Wright-Patterson AFB, OH 45433	
	LT C. Jazan	1
	R. R. Craig	1
	F. D. Stull	1